Journal of Molecular Graphics and Modelling 27 (2009) 584–589

Contents lists available at ScienceDirect

Journal of Molecular Graphics and Modelling

journal homepage: www.elsevier.com/locate/JMGM

A docking study of L-chicoric acid with HIV-1 integrase

Eamonn F. Healy [a,*], Jonathan Sanders [a], Peter J. King [b], W. Edward Robinson Jr.[c]

[a] Department of Chemistry, St. Edward's University, Austin, TX 78704, USA
[b] Department of Biology, St. Edward's University, Austin, TX 78704, USA
[c] Department of Pathology, University of California, Irvine, CA 92697, USA

ARTICLE INFO

Article history:
Received 21 May 2008
Received in revised form 18 September 2008
Accepted 22 September 2008
Available online 2 October 2008

Keywords:
L-Chicoric acid
HIV-1 integrase
Ligand binding
α,β-Unsaturated ester
Conformational analysis
AM1
Ab initio

ABSTRACT

Human immunodeficiency virus 1 integrase (HIV-1 IN) is the enzyme responsible for integrating the viral DNA into the host genome, and is essential to the replication of the virus. L-Chicoric acid (L-CA) is a bidentate catechol that has been identified as a potent inhibitor of HIV-1 IN. Using the new Autodock 4.0 free-energy function we have obtained a L-CA binding mode that explains its observed potency and is consistent with available experimental data. Because of the α,β-unsaturated ester functionality of the side arms of L-CA we first performed an extensive conformational analysis of L-CA using semiempirical and *ab initio* calculations. As a result we have identified two distinct L-CA binding modes, one for the *s-cis*/*s-cis* and another for *the s-cis*/*s-trans* isomers. The most stable conformer was found to be the structure with the α,β-unsaturated ester in the *s-cis* conformation for both arms of L-CA. This conformer also gave the top-ranked docking solution. Analysis of the interactions with key IN residues, combined with results using a L-CA tetraacetylated derivative and a Q148A IN mutant, correlate well with the experimental data.

1. Introduction

Human immunodeficiency virus 1 integrase (HIV-1 IN), the enzyme responsible for integrating the viral DNA into the host genome, is proving a fertile area of investigation using rational drug design methodology, and the first drug of this type has been approved for treatment under the generic name Raltegravir [1]. This inhibitor is broadly related to the diketo acids (DKA), molecules that function as strand-transfer inhibitors. L-Chicoric acid (L-CA, Fig. 1) shares a common binding pocket with the DKAs but is significantly larger than the DKAs, and as such has substantially more contact residues within the active site. As such it represents an optimal probe of IN catalytic activity. In addition IN mutations investigated to date show substantial cross-resistance to L-CA and certain DKAs, with many of the remainder exhibiting dramatically reduced inhibition by L-CA but little or no effect on the anti-IN activities of the DKA [2].

Although no structure of a full-length retroviral integrase has been published to date, the structures of isolated domains currently available reveal a common set of three domains with conserved three-dimensional folds and significant sequence similarity [3]. All known retroviral integrases contain the following domains: a zinc-binding N-terminal domain (H12, H16, C40 and C43), a catalytic core domain (D64, D116 and E152), and a dsDNA-binding C-terminal domain. DNA crosslinking studies have implicated residues H114, Y143, and K159 as being putatively involved in nucleic acid binding [4]. Within the active site, residue Q148 has been shown to interact with nucleic acid and is conserved in all integrases. In addition, the active site contains a highly conserved unstructured loop implicated in binding DNA with a 'hinge' formed by two immutable glycines (G140 and G149) [5]. A bound metal atom (Mn^{2+} or Mg^{2+}) is known to be necessary for wild-type HIV-1 IN activity [6,7]. Several partial integrase structures have been solved with bound inhibitors including 1-(5-chloroindol-3-yl)-3-(tetrazoyl)-1,3-propandione-ene (5CITEP, Fig. 1), a DKA[3].

Given the experimental data available for L-CA inhibition, and its utility in elucidating the structure of the HIV-1 IN binding site, it was felt that a thorough examination of its mode of binding was warranted. The restricted rotation due to α,β-unsaturated ester functionality present in L-CA presents a further impetus for an L-CA docking study.

2. Methodology

2.1. Ligands

Early molecular mechanics calculations for unsaturated aldehydes and ketones supported the common assumption that

* Corresponding author. Tel.: +1 512 448 8467; fax: +1 512 448 8492.
E-mail address: healy@stedwards.edu (E.F. Healy).

1093-3263/$ – see front matter © 2008 Elsevier Inc. All rights reserved.
doi:10.1016/j.jmgm.2008.09.011

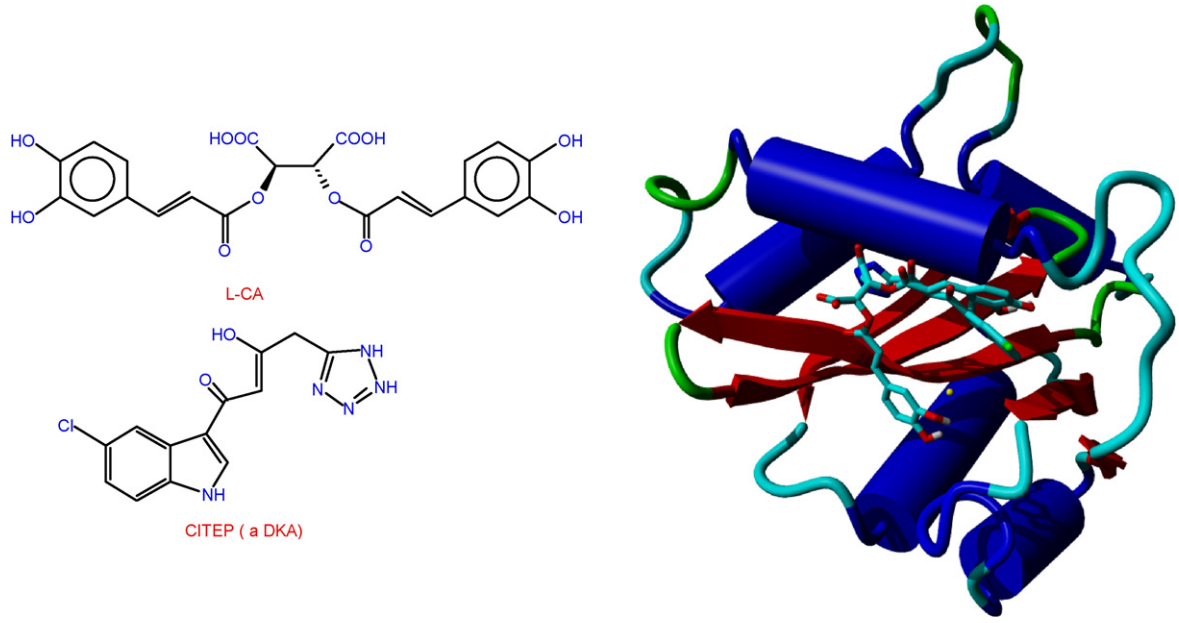

Fig. 1. Chemical structures for L-chicoric acid (L-CA) and CITEP, and a graphical representation of the catalytic domain of HIV-1 IN showing the predicted binding mode for L-CA and the experimental position if 5CITEP.

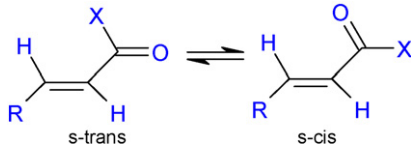

Fig. 2. Conformational isomerism in α,β-unsaturated carbonyl compounds.

conjugative stabilization favors the existence of only the *s-trans* conformer (Fig. 2) [8]. More recently *ab initio* calculations have provided support for the *s-cis* conformer being both more stable [9] and less stable [10] than the *s-trans* conformer. Raman and IR spectra of methyl *trans*-cinnamate (Fig. 2, R = Ph, X = OMe) measured as a function of temperature in both the solid and liquid phases led to the conclusion that the *s-cis* form was more stable and was the only conformer present in the solid [11]. More recently a lanthanide induced shift NMR (LIS/NMR) analysis was combined with molecular mechanics and *ab initio* calculations to give an experimental determination of the conformer energies and relative populations for a range of α,β-unsaturated aldehydes, ketones and esters [12]. For the molecule most closely resembling L-CA, methyl *trans*-cinnamate (Fig. 2, R = Ph, X = OMe) it was determined that the *s-cis* conformer was more stable by 0.41 kcal mol^{-1}, which corresponds to an *s-cis* conformer population of 68%.

The *ab initio* calculations accompanying the LIS/NMR analysis were performed at both the Hartree Fock (HF) level as well as utilizing the BL3YP hybrid functional. While the *s-cis* and *s-trans* energies agreed well with the experimental data, the geometries that correlated best with the experimentally observed chemical shifts were those optimized using molecular mechanics. Specifically, for methyl *trans*-cinnamate only the mechanics geometry that showed the methyl group staggered with respect to the CO plane and the ring 34° out of plane, in conjunction with an *s-cis*:*s-trans* ratio of 68:32 estimated from the calculated *ab initio* energies, gave good agreement with the experimentally observed δ values.

Based on this experience we optimized all the L-CA conformers with the AM1 semiempirical Hamiltonian [13], and then carried out single point energy calculations, at both the Hartree Fock (HF) and second-order Moller–Plesset correlation energy (MP2) level, on the lowest energy conformers. Based on pK_a values L-CA, and its derivatives, were modeled in the deprotonated state. Since it has been previously observed that the calculated conformer energies of molecules with two polar functional groups are solvent dependent [14] all calculations were performed with water as a solvent, as implemented in the polarisable continuum model (PCM) within Gaussian03 [15], and using the conductor-like screening model (COSMO) for the AM1 Hamiltonian. Our results are in good agreement with the earlier analysis of methyl *trans*-cinnamate, and indicate that the conformation where both arms of L-CA have the *s-cis* conformation is indeed the most stable. The conformations at all other rotatable bonds are essentially identical for all conformers identified in Table 1.

The general preference of esters and related compounds for the syn conformation, in preference to the anti-conformation, is generally attributed to steric interactions between the R and R′

Table 1
Relative energies, and predicted conformer populations, for the various L-CA conformer geometries optimized using the AM1 semiempirical model.

Isomer	E_{rel} (kcal mol^{-1})			% Population (T = 298 K)		
	AM1	HF/6-31G**	MP2/6-31G**	AM1	HF	MP2
cis–cis/syn–syn	0.0	0.0	0.0	75.6	77.3	74.9
cis–trans/syn–syn	1.2	1.2	1.1	24.2	21.6	23.9
trans–trans/syn–syn	3.7	2.6	2.5	0.2	1.1	1.2
cis–cis/syn–anti	6.0	5.5	10.9	$<1 \times 10^{-4}$	$<2 \times 10^{-4}$	$<2 \times 10^{-6}$

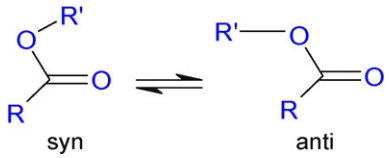

Fig. 3. Syn–anti isomerism in esters.

groups [16] (Fig. 3). While earlier data for methyl *trans*-cinnamate (Fig. 3, R′ = Me, R = [CH = CH–Ph]) suggested the possibility of substantial anti-conformer population [17], calculations performed as part of the LIS/NMR study gave a substantial ΔE (syn–anti) of between −9.0 and −12.4 kcal mol^{-1}. While our calculations for L-CA gave a slightly smaller energy difference, the anti-conformation is still significantly higher in energy, and as such only the syn–syn conformer is considered in the docking study. However semi-empirical calculations did indicate some flexibility for rotation around the C(=O)–O bond of the ester, as well as a low barrier to rotation around the C-Aryl bond. This latter result is consistent with the phenyl group torsion predicted for methyl *trans*-cinnamate [12].

AutoTors, as implemented in the Autodock tool kit (ADT) software program [18], was used to define the torsional degrees of freedom to be considered during the docking process. The number of flexible torsions defined for L-CA, and its derivative, was nine. Additionally the C(=O)–O bond of the ester was allowed to rotate ±15 relative to planarity, while the aryl rings were allowed to rotate ±45 relative to the planar conformation. Given the calculated conformer populations in Table 1 the L-CA ligand was initially restricted to the conformation where both arms are in a *s-cis* conformation. In an effort to reproduce a previous docking result for L-CA a *s-cis*/*s-trans* conformer was also docked. Finally atomic charges for L-CA were assigned using the Gasteiger–Marsili formalism [19], which is the type of atomic charges used in calibrating the AutoDock empirical free energy function [20].

In an experimental examination of the structural features responsible for the potency of L-CA against HIV-1 IN it was found that blocking the catechol functionality did increase the observed IC_{50}, but surprisingly still resulted in a fairly potent inhibitor [21]. We have also modeled the tetraacetylated derivative of L-CA that was used in this study.

2.2. Proteins

For the IN catalytic core domain, the structure obtained by X-ray analysis of the complex with 5CITEP was used (PDB 1QS4) [22]. For the purpose of docking, subunit A was selected, which is the only monomer in the asymmetric unit where the position of the ligand could be determined. The missing residues at positions 141–144 in this subunit were incorporated from monomer B of the IN structure after superposition of the backbones of residues 135–140 and 145–150. Polar hydrogens were added using the utility distributed with AutoDock 4.0 [23], and histidine residues were maintained unprotonated as previously determined to be appropriate [24]. The inserted loop residues and the hydrogen positions were subjected to a short energy minimization using the CHARMm force field as implemented in the Discovery Studio program suite. The solvation parameters used were the default values distributed with AutoDock 4.0. The grid maps representing the protein in the actual docking process were calculated with AutoGrid 4.0. The grid dimensions were chosen to be 30 Å × 30 Å × 30 Å, with a spacing of 0.375 Å between the grid points and the grid box centered on the C_α atom of catalytic residue aspartate 64. Autodock 4.0 is now parametrized for a variety of metals, including magnesium. The default atom types and parameters supplied with Autodock 4.0 were used throughout this study.

Previous work involving site-directed mutagenesis of selected residues within the IN binding pocket identified mutant IN proteins that were both attenuated for catalytic activity and resistant to inhibition by L-CA [2]. In an effort to validate our results for 1QS4 we also docked L-CA with a Q148A mutant, generated by simple replacement of glutamine 148 with alanine.

2.3. Docking

Docking was performed with version 4.0 of the program AutoDock, using the implemented empirical free energy function and the Lamarckian genetic algorithm [23]. Docking parameters included an initial population of 50 randomly placed individuals, a maximum number of 15 million energy evaluations, a maximum of 27,000 generations, a mutation rate of 0.02, a crossover rate of 0.80, and an elitism value of 1. Proportional selection was used, where the average of the worst energy was calculated over a window of the previous 10 generations. For the local search, the pseudo-Solis and Wets algorithm was applied using a maximum of 300 iterations per local search. The probability of performing local search on an individual in the population was 0.06, and the maximum number of consecutive successes or failures before doubling or halving the local search step size was 4. One hundred independent docking runs were carried out for each ligand, and results differing by less than 1.5 Å in positional root mean-square deviation (rmsd) were clustered together and represented by the result with the most favorable free energy of binding. The best docked conformations were those found to have the lowest binding energy and the greatest number of members in the cluster, indicating good convergence. We feel that increasing the maximum number of energy calculations to 15×10^6 greatly facilitated both the convergence and clustering observed in Table 2. Both 1QS4 and the mutant Q148A were kept rigid during the docking process.

3. Results and discussion

The docking results for L-CA and its tetraacetylated derivative with both 1QS4 and Q148A are summarized in Table 2. As noted before good convergence was achieved, with the best-docked conformations also those found to have the lowest binding energy and the greatest number of conformations per cluster. For the most

Table 2
Results of 100 independent docking runs for the ligands L-CA and its tetraacetylated derivative with proteins 1QS4 and the mutant Q148A.

Ligand	IN Protein	Cluster Occ.[a]	ΔG_{bind} (kcal mol^{-1})	K_i (μM)	IC_{50} (relative)[b]	H-bonded residues
L-CA (*s-cis*/*s-cis*)	1QS4	44	−8.1	1.1	1	D116, Q148, K156, K159
L-CA (*s-cis*/*s-trans*)	1QS4	29	−7.6	2.6	1	T66, H67, D92, Q148, K156, K159
L-CA (*s-cis*/*s-cis*)	Q148A	27	−6.2	31.7	20	D116, A148, K156
L-CA tetraacetylated (*s-cis*/*s-cis*)	1QS4	33	−6.6	14.0	9	T66, H67, Q148, K156, K159

[a] Number of individuals in the top-ranked cluster.
[b] The relative values for L-CA with 1QS4 and Q148A are from Ref. [2] and the values for the tetraacetylated derivative of L-CA with 1QS4 are from Ref. [21].

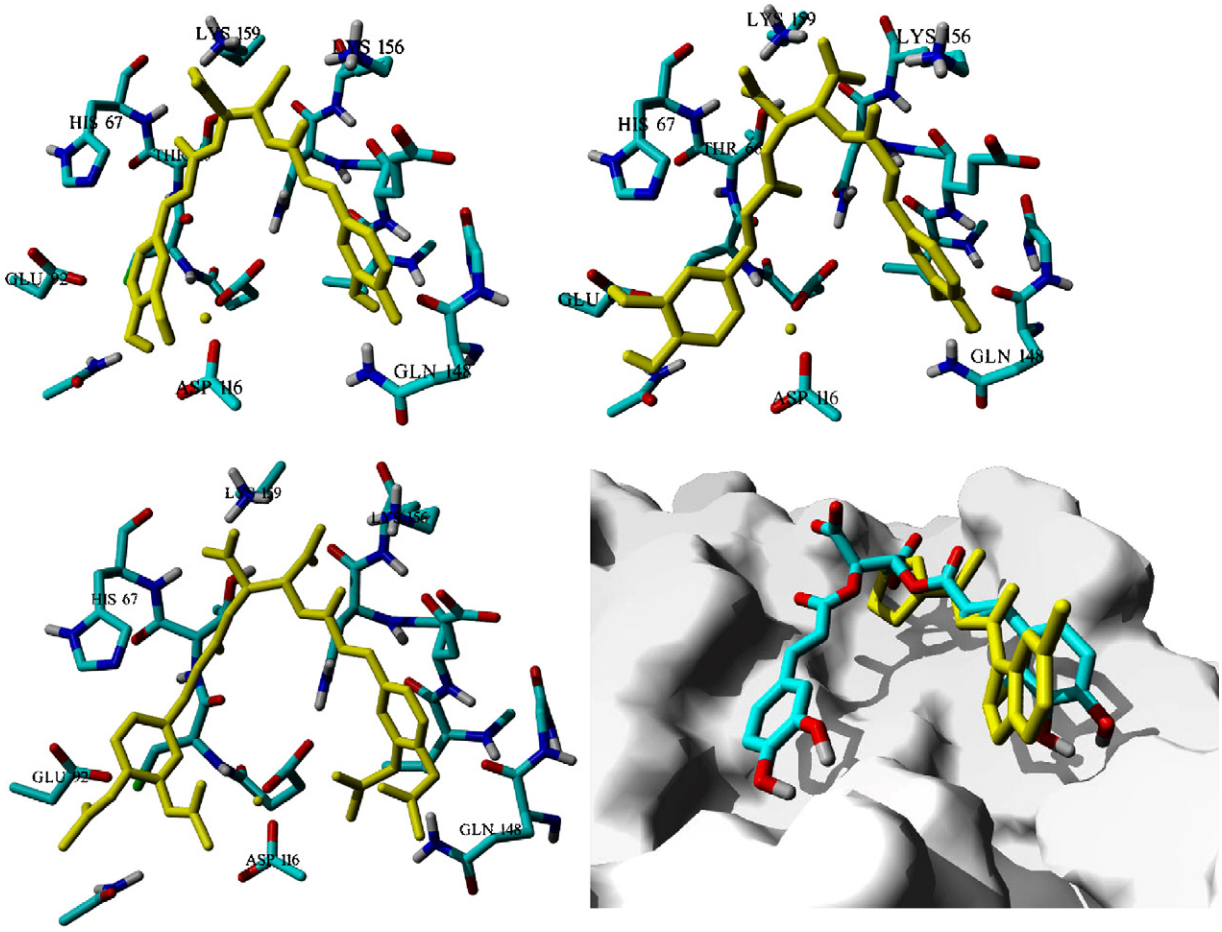

Fig. 4. Graphical representation of the top-ranked binding modes for *s-cis*/*s-cis* L-CA (a), s-*cis*/*s-trans* L-CA (b), tetraacetylated derivative of L-CA (c) and a surface image of the inhibitor binding pocket with bound *s-cis*/*s-cis* L-CA overlaid with the experimentally observed 5CITEP inhibitor (d).

stable conformer, with the α,β-unsaturated ester in the *s-cis* conformation for both arms of L-CA, 100 docking runs converged on a top-ranked cluster with a lowest energy binding mode as shown in Fig. 4(a). The predicted K_i is lower by a factor of two than the value reported in an earlier study [25]. Hydrogen bonds for all complexes were identified using the HBond Monitor utility as implemented in the Discovery Studio program suite. The default threshold value of 2.5 Å was used with a hydrogen bond angle of 120–180°. As can be seen from the surface image in Fig. 4(d) one arm of L-CA occupies the same area as the DKA 5CITEP, while the other arm occupies the region adjacent to the catalytic aspartates and the metal cation. The ability of L-CA to occupy both of these binding sites has been previously cited as an explanation for its observed potency [26]. In an effort to reproduce the earlier result [25] we also docked a conformer of L-CA where one of the α,β-unsaturated esters is in an *s-trans* arrangement. This conformation did converge on a top-ranked solution with a ΔG identical to the previously reported value of −7.6 kcal mol^{-1}, and a binding mode, Table 2 and Fig. 4(b), also similar.

Comparing the binding modes for the *s-cis*/*s-cis* and the *s-cis*/*s-trans* isomers reveals some important differences in the ligand protein interaction. Whereas one catechol ring of the *s-cis*/*s-trans* isomer shows extensive contact with glutamate 152 and hydrogen bonds with both the backbone and side chain of glutamine 148, the other ring is more exposed forming hydrogen bonds to glutamate 92. In addition there is hydrogen bonding with threonine 66 and histidine 67, but no observed interaction with the aspartate 116 catalytic residue. For the *s-cis*/*s-cis* isomer both arms of L-CA are well contained in the two binding pockets with both catechol rings forming hydrogen bonding networks with the glutamine 148 and aspartate 116 residues, respectively (Fig. 5). The interaction between the L-CA linker region and the lysine 156 and 159 residues are similar for both isomers. While the binding mode for the *s-cis*/*s-trans* isomer matches that reported in the earlier study, the hydrogen bonds between the *s-cis*/*s-cis* isomer and the catalytic aspartate 116 residue mirrors the binding mode observed in the docking study for the geminal disulfone analog of L-CA [27] (Fig. 6).

In an effort to validate the binding mode observed for the *s-cis*/*s-cis* isomer we also docked L-CA with a Q148A mutant of the IN catalytic domain, generated by simple replacement of glutamine 148 with alanine. By keeping the protein rigid during the docking no allowance was made for any conformational change that might occur due to such a substitution. Not surprisingly the predicted K_i for the binding of *s-cis*/*s-cis* L-CA with the Q148 mutant was substantially higher, by a factor of nearly 30, than that calculated for the 1QS4 protein. This predicted increase in K_i correlates well with the observed 20-fold increase in the IC_{50} for L-CA inhibition of the 3′-end processing reaction of the Q148A mutant [2], although of course care must be taken not to make any direct comparison between individual K_i and IC_{50} values (Table 2). Even with the substitution of alanine for glutamine some hydrogen bonding is observed with the backbone of residue 148.

Experimental IC_{50} values are also available for the inhibition of HIV-1 IN 3′-end processing by a tetraacetylated derivative of L-CA, a structure where no catechol hydroxyl protons are available for

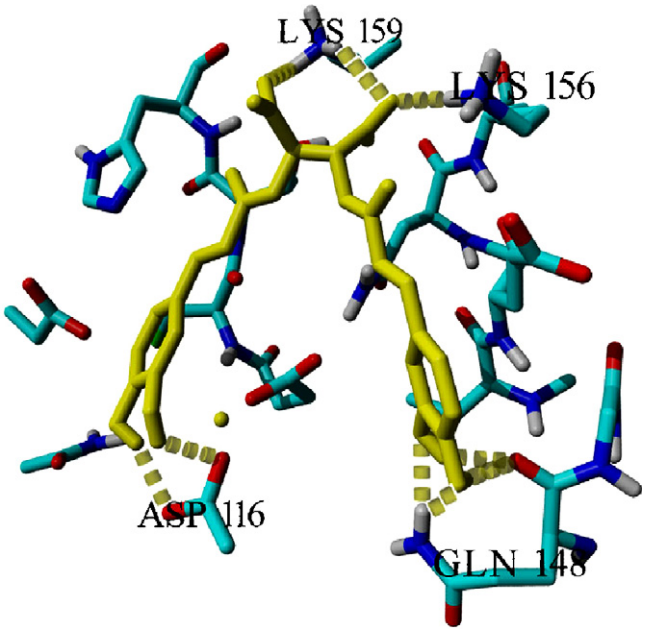

Fig. 5. Hydrogen bonded interactions for the top-ranked *s-cis/s-cis* L-CA solution.

hydrogen bonding. The 14-fold increase in K_i value predicted for docking with the 1QS4 protein, relative to L-CA, correlates well with the experimentally observed 9-fold increase in IC_{50}, relative to that observed for L-CA [21] (Table 2). Interestingly the preferred binding mode predicted for this tetraacetylated L-CA derivative is most similar to that found for the L-CA *s-cis/s-trans* isomer, with one catechol ring of L-CA again relatively exposed (Fig. 4(c)).

These results identify two general binding modes for L-CA, one where both catechol rings fit tightly in the two binding pockets and form multiple hydrogen bonds to the aspartate 116 and glutamine 148 residues, and a second where one of the catechol rings is relatively more exposed but does hydrogen bond to the aspartate 92 residue. The more effective binding mode does improve upon the previously reported binding strength [25], and the lower K_i value does correlate well with the observed potency of L-CA inhibition. The predicted loss of the hydrogen bonds from the L-CA catechol moiety to the glutamine 148 side chain explains the decrease in L-CA inhibition observed for the Q148A IN mutant. The flip to the conformation with the weaker binding mode predicted for the tetraacetylated L-CA derivative also correlates with the experimental observation that acetylation of the rings decreases L-CA inhibition but still yields a fairly potent inhibitor [21].

The HIV-1 IN system presents a substantial challenge for any docking study, not the least of these challenges being the fact that to date only the catalytic core domain has been structurally resolved. Additionally the active state of IN is a dimer and it has previously been shown that the crystallographic environment of the oligomeric state can influence the binding mode of IN inhibitors [28]. Finally the conformational variability of the catalytic loop, the unstructured region defined by the glycine hinges at positions 140 and 149, has been well established by large-scale dynamics studies [26], and combining molecular dynamics with flexible-ligand docking has revealed the existence of other potential binding regions [29]. Nevertheless the bidentate character of L-CA, allowing it to fit into two adjacent binding sites, presents a unique opportunity to explore the region adjacent to both the catalytic residues and the so-called catalytic loop. A combination of a thorough conformational analysis of the ligand and the new Autodock 4.0 free-energy function has yielded a L-CA binding mode that explains its observed potency and is consistent with available experimental data.

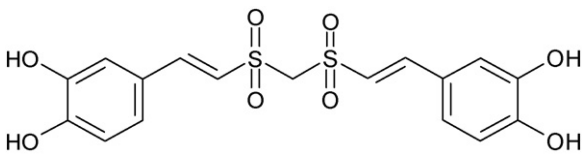

Fig. 6. Disulfone analog of L-CA.

Acknowledgements

The authors are grateful to the W.M. Keck Foundation grant for their generous support of this work. EFH and JS also wish to thank the Welch Foundation (Grant # BH-0018) for its continuing support of the Chemistry Department at St. Edward's University. We thank Dr. Arthur Olson for the Autodock 4.0 and Autogrid 4.0 programs, and for his help in implementing Autodock we would like to thank Dr. Sargis Dallakyan of the Scripps Research Institute.

References

[1] M. Markowitz, B.Y. Nguyen, E. Gotuzzo, F. Mendo, W. Ratanasuwan, C. Kovacs, G. Prada, J. Morales-Ramirez, C.S. Crumpacker, R.D. Isaacs, L.R. Gilde, Wan, H. Miller, M.D. Wenning, L.A. Teppler, H. Rapid, durable antiretroviral effect of the HIV-1 Integrase inhibitor Raltegravir as part of combination therapy in treatment-naive patients with HIV-1 infection: results of a 48-week controlled study, J. Acquir. Immune Def. Syndr. 46 (2007) 125–133.
[2] D.J. Lee, W.E. Robinson Jr., Preliminary mapping of a putative inhibitor-binding pocket for HIV-1 integrase inhibitors, Antimicrob. Agents Chemother. 50 (2006) 134–142.
[3] T.K. Chiu, D.R. Davies, Structure and function of HIV-1 integrase, Curr. Top. Med. Chem. 4 (2004) 965–977.
[4] T.M. Jenkins, D. Esposito, A. Engelman, R. Craigie, Critical contacts between HIV-1 Integrase and viral DNA identified by structure based analysis and photo-cross-linking, EMBO J. 16 (1997) 6849–6859.
[5] P.J. King, D.J. Lee, R.A. Reinke, J.G. Victoria, K. Beale, W.E. Robinson Jr., Human immunodeficiency virus type 1 integrase containing a glycine to serine mutation at position 140 is attenuated for catalysis and resistant to integrase inhibitors, Virology 306 (2003) 147–161.
[6] Y.-Q. Long, X.-H. Jiang, R. Dayam, T. Sanchez, S.S. Robert Shoemaker, N. Neamati, Rational, Design and synthesis of novel dimeric diketoacid-containing inhibitors of HIV-1 integrase: implication for binding to two metal ions on the active site of Integrase, J. Med. Chem. 47 (2004) 2561–2573.
[7] T.L. Diamond, F.D. Bushman, Role of metal ions in catalysis by HIV integrase analyzed using a quantitative PCR disintegration assay, Nucleic Acids Res. 34 (2006) 6116–6125.
[8] T. Liljefors, N. Allinger, Conformational analysis. CXII. Conformations, energies, and electronic absorption spectra of α,β-unsaturated aldehydes and ketones, J. Am. Chem. Soc. 98 (1976) 2745–2749.
[9] T. Egawa, S. Maekawa, H.F. Fujiwara, H. Takeuchi, S. Konaka, Molecular structure and conformation of methyl acrylate. A gas electron diffraction study augmented by ab initio calculation and rotational constants, J. Mol. Struct. (Theochem.) 353 (1995) 193–201.
[10] K.B. Wiberg, R.E. Rosenberg, P.R. Rablen, Butadiene 2. Examination of the energetic preference for coplanarity of double bonds. Comparison of butadiene, acrolein, and vinylamine, J. Am. Chem. Soc. 113 (1991) 2890–2898.
[11] J.R. Durig, T.S. Little, Conformational barriers to internal rotation and vibrational assignment of methyl vinyl ketone, J. Chem. Phys. 75 (1981) 3660–3666.
[12] R.J. Abraham, M. Mobli, J. Ratti, F. Sancassan, T.A.D. Smith, A Modelling and LIS/NMR investigation of the conformations of α,β-unsaturated carbonyl compounds., J. Phys. Org. Chem. 19 (2006) 384–392.
[13] M.J.S. Dewar, E.G. Zoebisch, E.F. Healy, J.J.P. Stewart, AM1: a new general purpose quantum mechanical molecular model, J. Am. Chem. Soc. 107 (1985) 3902–3909.
[14] F. Yoshinaga, C.F. Tormena, M.P. Freitas, R. Rittner, R.J. Abraham, Conformational analysis of 2-halocyclohexanones: an NMR, theoretical and solvation study, J. Chem. Soc. Perkin Trans. 2 (2002) 1494–1498.
[15] M.J. Frisch, G.W. Trucks, H.B. Schlegel, G.E. Scuseria, M.A. Robb, J.R. Cheeseman, J.A. Montgomery Jr., T. Vreven, K.N. Kudin, J.C. Burant, J.M. Millam, S.S. Iyengar, J. Tomasi, V. Barone, B. Mennucci, M. Cossi, G. Scalmani, N. Rega, G.A. Petersson, H. Nakatsuji, M. Hada, M. Ehara, K. Toyota, R. Fukuda, J. Hasegawa, M. Ishida, T. Nakajima, Y. Honda, O. Kitao, H. Nakai, M. Klene, X. Li, J.E. Knox, H.P. Hratchian, J.B. Cross, V. Bakken, C. Adamo, J. Jaramillo, R. Gomperts, R.E. Stratmann, O. Yazyev, A.J. Austin, R. Cammi, C. Pomelli, J.W. Ochterski, P.Y. Ayala, K. Morokuma, G.A. Voth, P. Salvador, J.J. Dannenberg, V.G. Zakrzewski, S. Dapprich, A.D. Daniels, M.C. Strain, O. Farkas, D.K. Malick, A.D. Rabuck, K. Raghavachari, J.B. Foresman, J.V. Ortiz, Q. Cui, A.G. Baboul, S. Clifford, J. Cioslowski, B.B. Stefanov, G. Liu, A.

Liashenko, P. Piskorz, I. Komaromi, R.L. Martin, D.J. Fox, T. Keith, M.A. Al-Laham, C.Y. Peng, A. Nanayakkara, M. Challacombe, P.M.W. Gill, B. Johnson, W. Chen, M.W. Wong, C. Gonzalez, J.A. Pople, Gaussian 03. Revision C. 02, Gaussian, Inc., Wallingford, CT, 2004.

[16] D.M. Pawar, A.A. Khalil, D.R. Hooks, K. Collins, T. Elliott, J. Stafford, L. Smith, E.A.E. Noe, *Z* conformations of esters thiol esters and amides, J. Am. Chem. Soc. 120 (1998) 2108–2112.

[17] N. Shida, C. Kabuto, T. Niwa, T. Ebata, Y. Yamamoto, Studies on *s-cis*/*s-trans* preference of acyclic α,β-unsaturated esters. Reactions, supersonic jet spectroscopy, NOEs, and X-ray analysis, J. Org. Chem. 59 (1994) 2108–4075.

[18] AutoDock Tools, http://www.autodock.scripps.edu/resources/adt/index_html.

[19] J. Gasteiger, M. Marsili, Iterative partial equilization of orbital electronegativity—a rapid access to atomic charges, Tetrahedron 36 (1980) 3219–3228.

[20] G.M. Goodsell, D.S. Halliday, R.S. Huey, R. Hart, W.E. Belew, R.K. Olson, A.J. Olson, Automated docking using a Lamarckian genetic algorithm and an empirical binding free energy function, J. Comput. Chem. 19 (1998) 1639–1662.

[21] Z. Lin, N. Neamati, H. Zhao, Y. Kiryu, J.A. Turpin, C. Aberham, K. Strebel, K. Kohn, M. Witvrouw, C. Pannecouque, Z. Debyser, E. De Clercq, W.G. Rice, Y. Pommier, T.R. Burke Jr., Chicoric acid analogues as HIV-1 integrase inhibitors, J. Med. Chem. 42 (1999) 1401–1414.

[22] Y. Goldgur, R. Craigie, G.H. Cohen, T. Fujiwara, T. Yoshinaga, T. Fujishita, H. Sugimoto, T. Endo, H. Murai, D.R. Davies, Structure of the HIV-1 integrase catalytic domain complexed with an inhibitor: a platform for antiviral drug design, Proc. Natl. Acad. Sci. U.S.A. 96 (1999) 13040–13043.

[23] R. Huey, G.M. Morris, A.J. Olson, D.S. Goodsell, A semiempirical free energy force field with charge-based desolvation, J. Comput. Chem. 28 (2007) 145–152.

[24] M.L. Barreca, K.W. Lee, A. Chimirri, J.M. Briggs, Molecular dynamics studies of the wild type and double mutant HIV-1 integrase complexed with the 5CITEP inhibitor, Biophys. J. 84 (2003) 1450–1463.

[25] C.A. Sotriffer, H. Ni, J.A. McCammon, Active site binding modes of HIV-1 integrase inhibitors, J. Med. Chem. 43 (2000) 4109–4117.

[26] M.C. Lee, J. Deng, J.M. Briggs, Y. Duan, Large-scale conformational dynamics of the HIV-1 integrase core domain and its catalytic loop mutants, Biophys. J. 88 (2005) 3133–3146.

[27] D.C. Meadows, D.J. Tantillo, J. Gervay-Hague, Correlation of biological activity with active site binding modes of geminal disulfone HIV-1 integrase inhibitors, Chem. Med. Chem. 1 (2006) 959–964.

[28] C.A. Sotriffer, H. Ni, J.A. McCammon, HIV-1 integrase inhibitor interactions at the active site: prediction of binding modes unaffected by crystal packing, J. Am. Chem. Soc. 122 (2000) 6136–6137.

[29] J.R. Schames, R.H. Henchman, J.S. Siegel, C.A. Sotriffer, H. Ni, J.A. McCammon, Discovery of a novel binding trench in HIV integrase, J. Med. Chem. 47 (2004) 1879–1881.